Technical paper

Nanocomposite Foams from Iron Oxide Stabilized Dicyclopentadiene High Internal Phase Emulsions: Preparation and Bromination

Sebastijan Kovačič,[1,4]* Nadejda B. Matsko,[2] Gregor Ferk[3] and Christian Slugovc[1]

[1] *Graz University of Technology, Institute for Chemistry and Technology of Materials, Stremayrgasse 9, A 8010 Graz, Austria*

[2] *Graz Center for Electron Microscopy (FELMI-ZFE), Stremayrgasse 17, A 8010 Graz, Austria*

[3] *University of Maribor, Faculty of Chemistry and Chemical Engineering, Smetanova 17, SI-2000 Maribor, Slovenia*

[4] *National Institute of Chemistry, Hajdrihova 19, 1000 Ljubljana, Slovenia*

* *Corresponding author: E-mail: sebastijan.kovacic@ki.si*

Received: 04-10-2013

Abstract

Nanocomposite polyHIPE foams with open-cellular morphology were obtained using nanoparticles ($\gamma Fe_2O_3/Fe_3O_4$), surfactant (Pluronic L121) or nanoparticle/surfactant stabilized dicyclopentadiene high internal phase emulsions (DCPD HIPEs). Upon curing, cavity sizes were found to vary drastically between 950 ± 360 μm down to 7 ±3 μm depending on the HIPE formulations. As-obtained nanocomposite polyHIPE foams were functionalized using elemental bromine in THF. Upon bromination the nanoparticles are moved from the cavities surfaces into the bulk phase of the polymer scaffold, which affects the inductive-heating capability of the magnetic nanocomposite foams decreasing it by the factor of 2.

Keywords: Pickering HIPEs, $\gamma Fe_2O_3/Fe_3O_4$ nanoparticles, Ring Opening Metathesis Polymerization (ROMP), Dicyclopentadiene, Inductive heating

1. Introduction

Emulsions represent one of the most important classes in colloid science and particularly macro-dispersed High Internal Phase Emulsions (HIPEs)[1] became a versatile type of emulsions for the preparation of well-defined open porous polymers, termed as polyHIPEs. For surfactant-stabilised HIPEs, the major challenge to prepare stable water-in-oil (W-in-O) or oil-in-water (O-in-W) emulsions is to find a suitable stabiliser which is selectively soluble in either of the immiscible liquids, referred to as phases. In an emulsion one phase (the internal phase) is dispersed as droplets within the other phase (the continuous phase). Usually large fractions of the stabilizer (5–50 wt. % of the organic phase) are required to stabilise HIPEs effectively. [2] Polymerization of the continuous phase of HIPEs and removal of the droplets of the dispersed phase used as a so called soft template, leads to the solid macroporous polyHIPEs foams (**PHF**). The morphology of PHF is hierarchically structured consisting of large cavities (in the range of 1–100 μm) connected via smaller windows (typically one fourth of the cavity size).[3] As emulsions with a volume fraction of the internal (droplet) phase higher than 74%, the stabilization of HIPEs represents a challenge in the formation process during which phases can macroscopically phase separate.[4]

Particle stabilization is a good alternative to the surfactant stabilized emulsions, as it yields surfactant-free emulsions and brings in additional properties to the final composite material.[5] The ability of particles to stabilize emulsions was recognized by the W. Ramsden in 1903 followed by the statement “solid matter has the power of forming persistent emulsions”.[6] However, S. U. Pickering was the first who published an extensive study on particle-stabilized emulsions hence the term “Pickering emulsions” is nowadays used.[7] Particles are irreversibly adsorbed at the interface between two immiscible liquids due

to their high energy of attachment (thousands of *kT*/particle), forming a shell around droplets that protects emulsions against droplet coalescence due to their high kinetic stability.[8] A number of factors affect the stabilization of Pickering emulsions, wherein the particles' wettability (often expressed as a contact angle),[9] size and shape of the particles[10] and their concentration[11] were found to be crucial. Among all factors, particle adsorption at the interface is largely determined by the extent to which the particle is wetted by the phases. Wettability is a measure for the extent of wetting of a solid by a particular liquid (i.e. how a liquid spreads on the surface of the solid). Wettability is quantified by reference to the contact angle (θ) that the solid forms with the liquid, with a low č indicating high wettability and a high θ indicating low wettability.[12] Due to the favourable characteristics of Pickering emulsions also HIPEs (either W-in-O or O-in-W) were obtained using particle stabilization. TiO_x, SiO_x and Fe_2O_3/Fe_3O_4 nanoparticles modified with oleic acid were used to stabilize HIPEs wherefrom poly Pickering foams with up to 92 % of porosity were successfully obtained.[13] Also silane modified SiO nanoparticles or 12-acryloxy-9-octadecenoic acid modified $F^e{}_2O_3/Fe_3O_4$ nanoparticles were used to stabilized HIPEs and poly Pickering foams with up to 90 % of porosity were obtained.[14] Beside solid inorganic nanoparticles also polymer particles,[15] carbon nanotubes,[16] and bacterial cellulose[17] were used as emulsifiers and were shown to effectively stabilize W-in-O Pickering HIPEs. Recently, reversed O-in-W Pickering HIPEs arose as an alternative to the W-in-O Pickering HIPEs stabilized by soft microgel nanoparticles,[18] poly(urethan urea) nanoparticles,[19] hydroxyapatite nanoparticles,[20] protein nanoparticles,[21] or cellulose nanocrystals.[22] However, the most important feature of PHF, i.e. fully interconnected morphology could not be retained. This effect can be avoided by the addition of small amounts of the surfactant in combination with said nanoparticles and interconnectivity can be obtained, with the nanoparticles possibly embedded in or on the polymer walls (*cf.* Fig. 1).[23,24] Using the co-stabilizing approach, polystyrene nanocomposite polyHIPE foams (**nPHF**) from MnO_2 were obtained and the catalytic activity of MnO_2 nanoparticles was studied.[25] Furthermore, nPHF from SiO and Fe_2O_3/Fe_3O_4 nanoparticles were also obtained and used to study their permeability[26] or self-heating properties.[27]

Materials based on the polymerization of dicyclopentadiene (DCPD) have gained a lot of attention lately, because of the cheap monomer, high modulus, ease of synthesis and the potential for polymer modification through the reaction with the olefins along the polymer backbone.[28] Our recently communicated approach for improving the rather poor mechanical properties of PHF is based on the preparation of poly(dicyclopentadiene) (polyDCPD) foams using Ring Opening Metathesis Polymerization[29] Such obtained open porous foams exhibit impressive mechanical properties[30,31,32,33] and offer several ways for further functionalization (either by conventional nucleophilic/electrophilic substitution/addition or more advanced iEDDA click reactions) leading to high loadings of functional groups in the foams (even up to 8 mmol/g of polymer).[34]

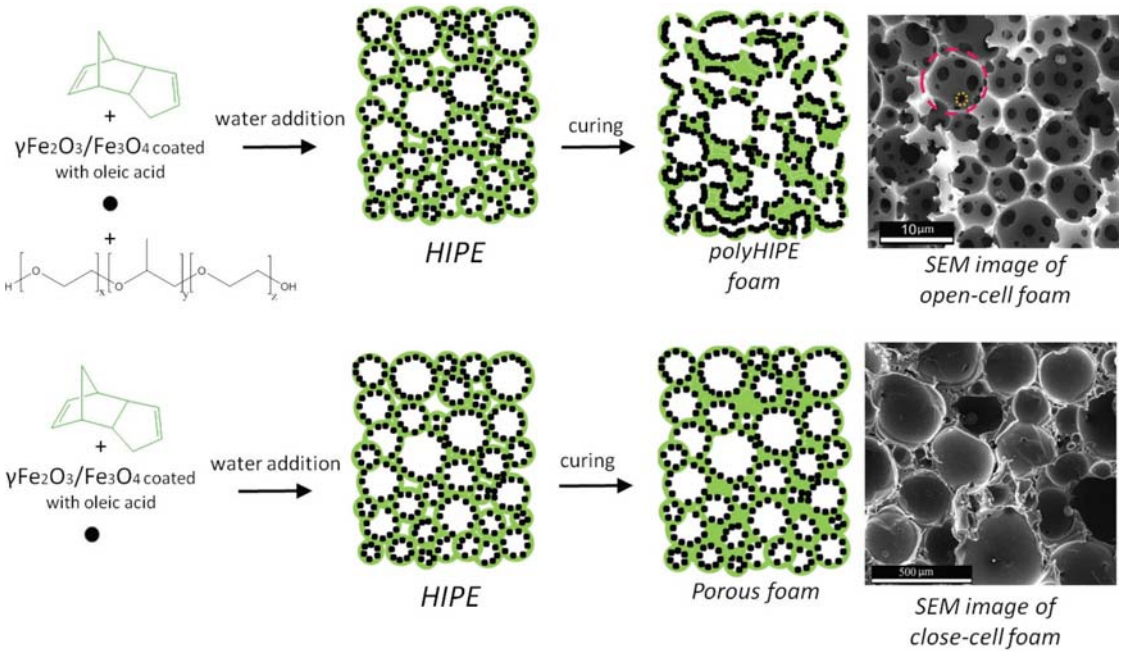

Figure 1. Preparation of nanocomposite foams: co-stabilized system (surfactant and nanoparticles) yielding open-cell foam morphology (upper row) and system without surfactant as co-stabilizer yielding closed-cell foam morphology (bottom row)

The excellent physical and chemical properties of polyDCPD could be immensely interesting regarding matrix materials in nanocomposite structures.[35] Therefore, the investigation of polyDCPD nanocomposites became of great interest.[36] Preparation, characterisation and possible applications of nanocomposite polyHIPE material from magnetic oleic acid coated $\gamma Fe_2O_3/Fe_3O_4$ nanoparticles (**FeO_x-NP**s) and polyDCPD were already discussed in a previous manuscript. As-obtained nanocomposite foams out from **FeO_x-NP**s were shown to produce heat when an alternating magnetic field was applied.[24,27] Such a non contact, magnetic induction hyperthermia has several advantages over conventional heating.[37] Our interest with **FeO_x-NP**s nanocomposite foams is focused on solid phase chemical syntheses as well as catalytic transformations using non contact heating approach that **FeO_x-NP**s can offer.[38] In the case when **FeO_x-NP**s within the nanocomposite foam provide heating during chemical syntheses or catalytic transformation, a placement away from the pore surface is beneficial. Therefore, control over the location of the nanoparticles in the nanocompostit foam is desirable. Reason for that lies in chemical sensitivity of **FeO_x-NP**s, which were found to oxidize in the presence of molecular oxygen losing their magnetic properties.[39]

Within the present technical article, we would like to present information regarding the sensitivity of **FeO_x-NP**s and how bromination of polyDCPD @ $\gamma Fe_2O_3/Fe_3O_4$ nanocomposites foams affects the magnetic induction hyperthermia of **FeO_x-NP**, which are embedded into the foam. Nanocomposite foams were functionalized using elemental bromine in a THF solution, whereby also the location of the nanoparticles within the material changed as a consequence of polyDCPD swelling in THF.

2. Experimental Section

2. 1. Materials

Dicyclopentadiene (**DCPD**, Aldrich), poly(ethylene glycol)-*block*-poly(propylene glycol)-*block*-poly(ethylene glycol) (Pluronic®L-121, Aldrich), (H_2IMes) (PCy_3) Cl_2Ru(3-phenyl-indenylid-1-ene), H_2IMes = N,N-bis(mesityl) 4,5-dihydroimidazol-2-yl), PCy_3 = tricyclohexylphosphine) (**M2**), bromine (p.a. Merck), tetrahydrofuran (Carel Roth), acetone (Sigma-Aldrich) were used as received.

2. 2. Synthesis and Modification of Nanoparticles

During the preparation of iron oxide nanoparticles (NPs), the mole ratio of Fe^{2+} to Fe^{3+}, the pH of the aqueous phase, the crystallization temperature, and the crystallization time are important factors influencing the size and magnetic properties of the obtained Fe_3O_4 NP. The iron oxide nanoparticles were synthesized according to a method described elsewhere.[40] The average diameter of iron oxide nanoparticles, prepared by co-precipitation and used for incorporation into HIPEs, was estimated from TEM images and was found to be approximately 16 nm, with a size distribution between 10 nm and 24 nm.

2. 3. Preparation of DCPD/$\gamma Fe_2O_3/Fe_3O_4$ HIPEs

For making DCPD/ **FeO_x-NP** HIPEs, we started with already disclosed formulation of DCPD HIPEs and additionally added dry $\gamma Fe_2O_3/Fe_3O_4$ NPs. DCPD and iron oxide NPs were mixed with an overhead stirrer for 1h at 600 rpm in a round-bottom flask and used as the oil (continuous) phase. Upon vigorous mechanical stirring at room temperature the internal (droplet) phase consisting of deionised water was slowly added drop wise over about 1 h. When all internal phase was added, the according amount of Pluronic® L121 was additionally added to the reactor in case of *system II* while in case of *system I* no additional surfactant was present (masses according to the Table 1). The stirring was prolonged for 1 h. After that, initiator **M2**, dissolved in 0.25 mL of toluene was added and the emulsion was stirred for 1 min. Subsequently, the emulsion was transferred to appropriate moulds (poly(styrene) containers, steel moulds or glass vials) and the filled moulds were transferred into a preheated oven operating under air. Curing of the emulsions at 80 °C for 4 h resulted in the formation of brown rigid monoliths in all cases. Referenced samples (without NPs) were prepared using the same protocol as described above according to the masses from Table 1. All specimens were purified by Soxhlet extraction with acetone. Upon drying in a desiccator under vacuum the preparation process was finished.

2. 4. Functionalization of DCPD@$\gamma Fe_2O_3/Fe_3O_4$ Nanocomposite Foams

In a typical bromination experiment, a piece of the **pDCPD-15w-10v** sample (4 g; 45.3 mmol of double bonds) was immersed in a solution of THF (200 mL) and bromine (2.26 mL). The nanocomposite was stirred in a solution for 24h at room temperature. Afterwards, the nanocomposite was washed with copious amounts of THF, acetone/THF and acetone in order to remove unreacted bromine. The sample was then dried under reduced pressure at 25 °C over night. Brominated sample that was investigated is marked as **pDCPD-15w-10v-Br.**

2. 5. SEM Characterization of Poly(DCPD)/ iron Oxide Nanocomposite PolyHIPEs

Morphology investigations were done by scanning electron microscopy (SEMs were taken on a JWS-7515, JEOL Ltd. microscope). Micrographs were taken at several magnifications between 2500 X to 7000 X, at 7 mm

working distance and 20 kV voltage applied. A piece of the each sample was mounted on a carbon tab for better conductivity and a thin layer of gold was sputtered on the sample's surface prior to scanning analysis.

2. 6. TEM Characterization of Poly(DCPD)/ iron Oxide Nanocomposites PolyHIPEs

The samples were embedded in Araldite/Epon embedding mixture which was composed of 49% w/w Araldite/Epon stock solution, 49% w/w Hardener DDSA (Fluka) and 2% w/w Accelerator DMP-30 (Fluka). Infiltration was performed stepwise (impregnation at room temperature for 24 h, and polymerisation at 50 °C for 72 hr.). Ultrathin sections (10–50 nm) were obtained using a Leica Ultracut E microtome (Leica, Austria) equipped with a diamond blade (Diatome, Switzerland). Sections for TEM analysis were collected on carbon coated grids, and examined in Philips CM 20 (Philips/FEI, Eindhoven) electron microscopes at 200 kV accelerating voltage. No staining was applied. All EDX experiments were performed in STEM mode with a probe current of 20 nA and a beam diameter of 100 nm, whereas EFTEM were done in TEM mode.

2. 7. Inductive Heating of Nanocomposites

A home-made system (*cf.* Fig. S6) was used to generate an alternating magnetic field with nominal field strength of 4.5 kA/m and a maximum frequency of 104 kHz. The setup consisted of five units: a variable sine wave function generator, a RF power amplifier, an induction coil, an oscilloscope and a digital voltmeter for temperature measurements using a PT100 sensor were used. The AC magnetic field was measured with a pickup coil positioned in the centre of the supply coil. For the thermal measurements of the magnetic material losses a sample of magnetic polyHIPE foam was placed in a glass vial in the centre of the surrounding supply coil. The length of the coil was twice the length of the glass vial in order to ensure a homogeneous field at the centre of the vial. The glass vial was placed in a heat-insulating poly(styrene) jacket to reduce heat dissipation from sample to the surroundings and vice versa. To further prevent temperature disruption from the surroundings, a vacuum tube was placed between sample protected with insulating poly(styrene) and the surrounding supply coil. The magnetic induction hyperthermia was measured on brominated and non-brominated nanocomposite samples of cylindrical shape with dimensions: 10 cm height, 1 cm in diameter having a hole in the middle to host the temperature sensor.

3. Results and Discussion

W-in-O DCPD HIPEs used in the present study were stabilized by different weight percentages of oleic acid covered iron oxide NPs (*i.e.* 1, 5, 10, 20 w% with respect to DCPD), without (*system I*) or with (*system II*) Pluronic L121 as the co-stabilizer (*cf.* Fig. 1 and Table 1). After the addition of water, the emulsions were further stirred for 1 h and the toluene solution of the initiator **M2** (0.0067 mol% with respect to DCPD) was added. Afterwards, the HIPEs were poured into moulds and transferred to an oven for 4 h at 80 °C. In all cases, the resulting monoliths were extracted for 24 h with acetone in a Soxhlet apparatus and dried under vacuum. In SEM both systems showed an open-cell structured morphology, typical for polyHIPE foams, with cavities and windows of different sizes.

Table 1. Emulsion compositions

sample	m (DCPD) [g]	m (M2) [mg]	FeO_x-NPs [g]	FeO_x-NPs [w %]	Surf. [vol. %]	V(H_2O) [mL]	Br [mL]
pDCPD-1w	1.30	1.30	0.014	1	/	5	/
pDCPD-5w	1.30	1.30	0.067	5	/	5	/
pDCPD-10w	1.30	1.30	0.150	10	/	5	/
pDCPD-15w	1.30	1.30	0.230	15	/	5	/
pDCPD-20w	1.30	1.30	0.330	20	/	5	/
pDCPD-1w-1.5v	8.02	8.02	0.083	1	1.5	33	/
pDCPD-5w-1.5v	8.08	8.08	0.430	5	1.5	33	/
pDCPD-10w-1.5v	8.01	8.04	0.830	10	1.5	33	/
pDCPD-15w-1.5v	8.06	8.08	1.450	15	1.5	33	/
pDCPD-20w-1.5v	8.06	8.06	2.050	20	1.5	33	/
pDCPD-1w-10v	8.06	8.06	0.083	1	10	33	/
pDCPD-5w-10v	8.01	8.02	0.430	5	10	33	/
pDCPD-10w-10v	8.06	8.05	0.830	10	10	33	/
pDCPD-15w-10v	8.06	8.05	1.450	15	10	33	/
pDCPD-20w-10v	8.06	8.08	2.050	20	10	33	/
pDCPD-15w-10v_Br	8.06	8.08	1.450	15	10	33	2.26
pDPCD-1.5v	1.30	1.33	/	/	1.5	5.5	/
pDPCD-10v	1.30	1.33	/	/	10	5.5	/

In contrast, *system I* yielded macroscopically observable pores with dimensions of 265 ± 100 μm up to 950 ± 360 μm (*cf.* Fig. 2A and *ref.*). Window formation took place in both systems and was most pronounced in sample p-DCPD-15w for system *I*, where windows with a diameter of 70±30 μm were formed all over the cavities. Actually, window formation in true Pickering polyHIPE foams (obtained from Pickering HIPEs stabilized solely with nanoparticles) is rather uncommon; these foams should exhibit mostly closed-cell morphologies.[13,14] On the other hand, s*ystem II* yielded cavities fully interconnected by the windows of sizes from 1.4 μm up to 5.1 μm. Cavity sizes range from 23 ± 10 μm up to 31 ± 16 μm, for samples stabilized with 1.5 v% of the surfactant (*cf.* Fig. 2B) and from 7 ± 3 μm up to 12 ± 7 μm for samples stabilized with 10 v% of the surfactant used (*cf.* Fig. 2C). Addition of the surfactant to the *system I* distinctly decreases cavity sizes, from 550 μm on average in case of *system I*, down to 23 ± 10 μm or 7 ± 3 μm on average for *system II* (*cf.* Fig. S2 and S3). For comparison, samples prepared without **FeO_x-NPs** were characterized by a cavity diameter of 10 ± 3 μm for 1.5 v% or 5 ± 2 μm for 10 v% surfactant stabilized HIPEs and with windows diameter of 2.0 ± 0.8 μm or 1.0 ± 0.5 μm respectively, i.e. 2–3 folds smaller than in case of presence of **FeO_x-NP**s (*cf.* Fig S4 and S5). From that observation, we can conclude that cavity sizes are tunable by the surfactant amount while the amount of **FeO_x-NP**s does not have an impact on the cavity sizes. The skeleton morphology was further investigated using TEM microscopy in order to determine the distribution of the **FeO_x-NP**s within the composite materials. In *system I*, **FeO_x-NP**s were found on the surface as well as in the bulk of the nanocomposite foam. **FeO_x-NP**s located in the bulk are mainly concentrated in islands of about 2 μm in size (biggest dimension) and only a minor amount of **FeO_x-NP**s is evenly distributed within the polyDCPD matrix (*cf.* Fig. 2D). More surprising was the finding in *system II,* where the vast majority of all **FeO_x-NP**s were found close to the surface of the cavities (*cf.* Fig. 2E, F).

In order to determine the amount of NPs embedded in the polymer matrix, thermogravimetric analysis (TGA) was performed. The residual mass after having heated the nanocomposites in a pure oxygen atmosphere with a heating rate of 10 °C/min to 550 °C increased from 5 w% in case of **pDCPD_10v_5w** to 15.6 w% in case of **pDCPD_10v_20w** (*cf.* Fig. S7).

In our previous studies, we have discussed functionalization of the pDCPD foams by showing thiol-ene reactions using un-oxidized pDCPD foams, imine reaction using oxidized pDCPD foams or iEDDA click reactions. Moreover, scope and limitations of bromination was studied on highly macroporous pDCPD membranes.[41] In the present technical article, the effect of bromination on the magnetically inductive heating capabilities of nanocomposite pDCPD/**FeO_x-NP**s foams is presented. Sample **pDCPD-15w-10v** obtained *via* system *II*

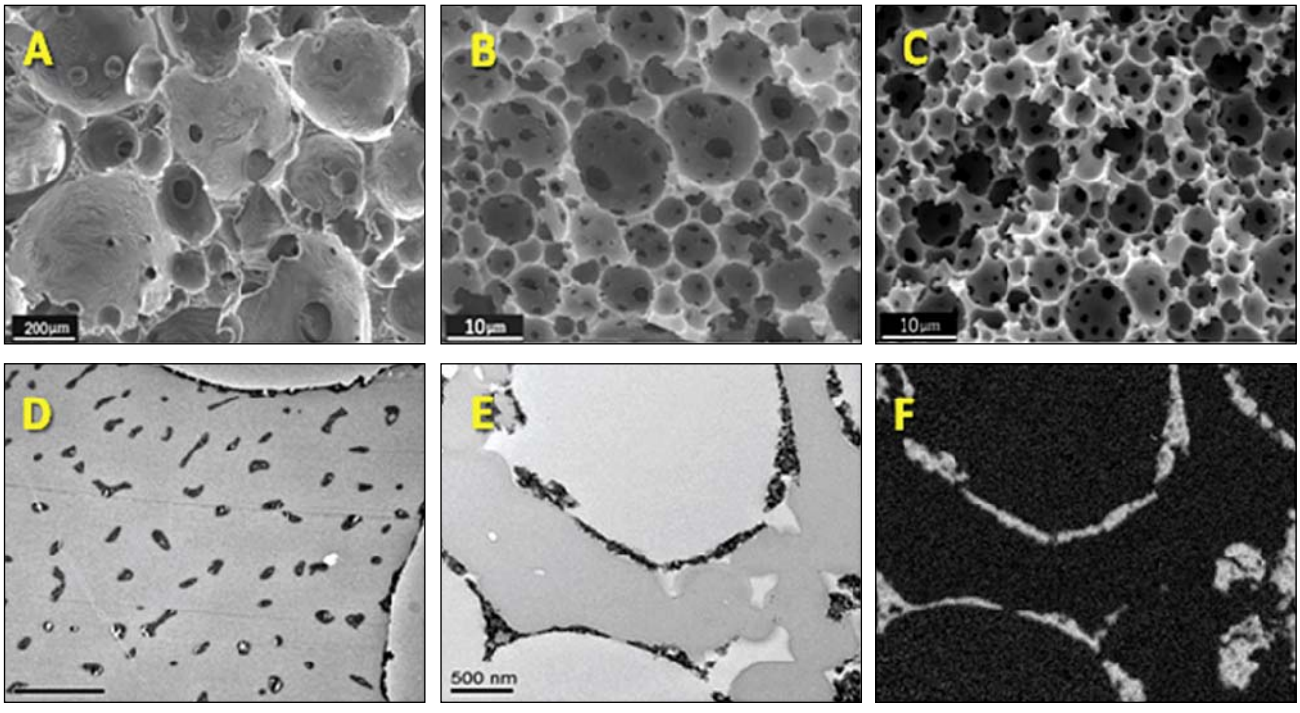

Figure 2. Upper row from left to the right: SEM images of nanocomposite foams obtained with 15 w% of **FeO_x-NP**s and: without surfactant – sample **pDCPD-15w** (image A), with 1.5 v% of the surfactant – sample **pDCPD-15w-1.5v** (image B) and with 10 v% of the surfactant – sample **pDCPD-15w-10v** (image C); bottom row from left to the right: TEM image of the **pDCPD-15w** sample (image D); TEM bright field image of the **pDCPD-15w-10v** sample (image E) and EFTEM iron jump ratio map image of the **pDCPD-15w-10v** (image F)

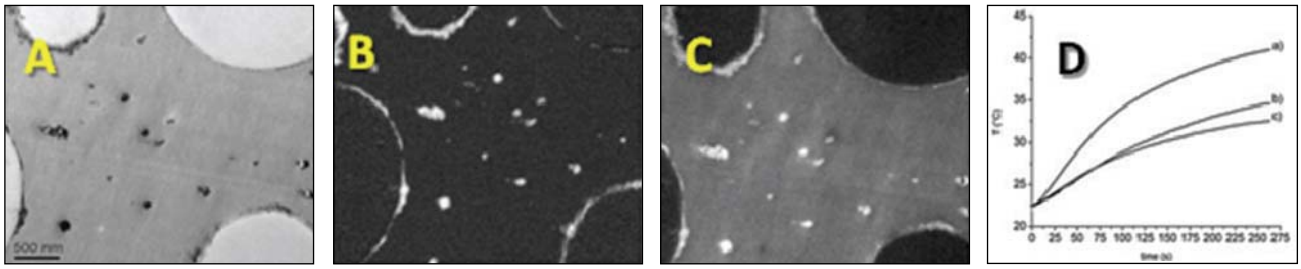

Figure 3. From left to the right: TEM bright field image of sample **pDCPD-15w-10v-Br** (image A), EFTEM bromine jump ratio map image of the sample **pDCPD-15w-10v-Br** (image B), EFTEM iron jump ratio map of the sample **pDCPD-15w-10v-Br** (image C) and inductive heating diagram (image D) of (a) DCPD-15w-10v sample, (b) DCPD-15w, (c) DCPD-15w-10v-Br

were used for bromination, where nanoparticles before bromination were found exclusively on the surface of cavities (*cf.* Fig. 2E). **pDCPD-15w-10v** was immersed in the THF/bromine solution for 24h, washed with copious amounts of THF and acetone and dried under the vacuum (*cf.* Fig. S8). Upon mapping of the thin section of the **pDCPD-15w-10v-Br** sample using energy filtered TEM (EFTEM), scanning TEM (STEM) and EDX analysis (*cf.* Fig S9), bromine was found all over the material (*cf.* Fig. 3B, 3C).

Yet it was investigated how bromination affects the self-heating capability of the composite foams upon exposure to an external magnetic field. The inductive heating was tested on a brominated sample **pDCPD-15w-10v-Br** and non-brominated samples **pDCPD-15w-10v** and **pDCPD-15w.** All three samples were exposed to the external alternating magnetic field with field strength of 16 kA/m. The inductive heating tests showed the highest heating efficiency for the **pDCPD-15w-10v** sample (ΔT = 18 °C) following by **pDCPD-15w** sample with heating response of 11 °C (ΔT = 11 °C) while the brominated sample **pDCPD-15w-10v-Br** showed a temperature increase of only 9 °C (*cf.* Fig. 3D). The difference in heating response between the non-brominated samples **pDCPD-15w-10v** and **pDCPD-15w** was briefly described in our previous study[27] and was ascribed to the nanoparticles' distribution as well as agglomeration within the polymer matrix, as nanoparticles' agglomeration is known to be responsible for lower inductive heating efficiency through increasing dipolar interactions within the agglomerates.[42] The lower heating response of the brominated sample might be rather ascribed to a reaction of bromine with the nanoparticles.[39] Moreover, as revealed by TEM analysis, some nanoparticles were found to be agglomerated in the polymer phase after bromination (*cf.* Fig. 3A, B). The dislocation of nanoparticles from surface in the bulk can be best explain by the high swelling degree of polyDCPD in THF (THF uptake of more than 1000 w %)[41] whereby nanoparticles that are not chemically attached to the surface, re-locate from the surface into the polymer phase and starts to agglomerate which might be a second reason for the decrease of the self-heating capability.

4. Conclusions

Within the present technical article, the preparation of DCPD@$\gamma Fe_2O_3/Fe_3O_4$ nanocomposite foams using HIPE templating approach with an emphasis on post-polymerization bromination of as-obtained nPHF has been summarized. The sensitivity of **FeO_x-NP**s to bromination was confirmed, and led to a decrease in magnetic induction hyperthermia of brominated nanocomposites by the factor of 2. Moreover, re-location of **FeO_x-NP**s from the surface to the bulk phase of the polymer-skeleton during bromination was observed.

5. Acknowledgements

Financial support by the European Community (CP-FP 211468-2 EUMET) and VARTA Micro Innovation GmbH is acknowledged. M. Bekovič is thanked for the thermal measurements and A. Leitgeb for proof reading.

6. References

1. a) K. J. Lissant, Surfactant Science Series, Vol. 6, Emulsion and Emulsion Technology, Part 1, ed. K. J. Lissant, Marcel Deckker Inc., N.Y., **1974** (b) J. Esquena, C. Solans, *Emulsions and Emulsion Stability*, J. Sjöblom (Ed.), Marcel Dekker Inc., Amsterdam, **2006**
2. J. M. Williams, A. J. Gray, M. H. Wilkerson, *Langmuir*, **1990**, *6,* 437.
3. (a) M. Silverstein, *Prog. Polym. Sci.*, **2014,** *39,* 199–234 (b) I. Pulko, P. Krajnc, *Macromol. Rapid. Commun.* **2012**, *33,* 1731–1746.
4. N. R. Cameron, P. Krajnc, and M. S. Silverstein, *Colloidal Templating*, in: M. S. Silverstein, N. R. Cameron and M. A. Hillmyer (Eds.) *Porous Polymers*, John Wiley & Sons, Inc., Hoboken, NJ, USA, **2011**.
5. L. Chen, D. Rende, L. S. Schadler, R. Ozisik, *J. Mater. Chem. A*, **2013**, *1,* 3837–3850.
6. W. Ramsden, *Math. Phys. Eng. Sci.*, **1903**, *72,* 156–164.
7. S. U. Pickering, *J. Chem. Soc. Trans.* **1907**, *91,* 2001–2021.

8. (a) R. Aveyard, B. P. Binks, J. H. Clint, *Adv. Colloid. Interface. Sci.* **2003**, *100–102,* 503–546; (b) B. P. Binks, *Curr. Opin. Colloid. Interface. Sci.* **2002**, *7,* 21.
9. (a) B. P. Binks, S. O. Lumsdon, *Langmuir* **2000**, *16,* 8622–8631 (b) R. Aveyard, B. P. Binks, J. H. Clint, *Adv. Colloid Interface Sci.* **2003**, *100–102,* 503–546.
10. B. P. Binks, S. O. Lumsdon, *Langmuir* **2001**, *17,* 4540–4547.
11. B. P. Binks, S. O. Lumsdon, *Langmuir*, **2000**, *16,* 2539–2547.
12. Menner, A., Ikem, V., Bismarck, A. "Particle Stabilised High Internal Phase Emulsions", WO/2009/013500.
13. a) A. Menner, V. Ikem, M. Salgueiro, M. S. P. Shaffer, A. Bismarck, *Chem. Commun.* **2007**, *41,* 4274–4276 (b) V. O. Ikem, A. Menner, A. Bismarck, *Angew. Chem., Int. Ed.* **2008**, *47,* 8277–8279 (c) V. O. Ikem, A. Menner, A. Bismarck, *Langmuir* **2010**, *26,* 8836–8841 (d) Vílchez, A., Rodríguez-Abreu, C., Esquena, J., Menner, A., Bismarck, A. *Langmuir* **2011**, *27,* 13342–13352.
14. (a) I. Gurevitch, M. S. Silverstein, *J. Polym. Sci. A, Polym. Chem.* **2010**, *48,* 1516–1525 (b) I. Gurevitch, M. S. Silverstein, *Macromolecules*, **2011**, *44,* 3398–3409. (c) I. Gurevitch, M. S. Silverstein, *Soft Matter*, **2012**, *8,* 10378–10387. (d) T. T. Li, H. R. Liu, L. Zeng, S. Yang, Z. C. Li, J. D. Zhang, X. T. Zhou, *J. Mater. Chem.*, **2011**, *21,* 12865–12872.
15. (a) Colver, P. J., Bon, S. A. F. *Chem. Mater.*, **2007**, *19,* 1537–1539 (b) Guanqing, S., Zifu, L., Ngai, T. *Angew. Chem. Int. Ed.* **2010**, *49,* 2163–2166 (c) Zhang, S., Zhu, Y., Hua, Y., Jegat, C., Chen, J., Taha, M. *Polymer*, **2011**, *52,* 4881–4890
16. (a) A. Menner, R. Verdejo, M. Shaffer, A. Bismarck, *Langmuir*, **2007**, *23,* 2398–2403. (b) M. C. Hermant, B. Klumperman, C. E. Koning, *Chem. Commun.*, **2009**, 2738–2740.
17. J. J. Blaker, K.-Y. Lee, X. Li, A. Menner, A. Bismarck, *Green Chem.*, **2009**, *11,* 1321–1326.
18. Z. Li, T. Ming, J. Wang, T. Ngai*, Angew. Chem. Int. Ed.*, **2009**, *48,* 8490–8493
19. Y. Zhu, S. Zhang, Y. Hua, J. Chen, C. P. Hu, *Polymer*, **2010**, *51*, 3612–3617.
20. S. Zhou, A. Bismarck, J. H. G. Steinke, *J. Mater. Chem.*, 2012, *22,* 18824–18829.
21. Z. Li, M. Xiao, J. Wang, T. Ngai, *Macromol. Rapid Commun.*, **2013**, *34*, 169–174.
22. I. Capron, B. Cathala, *Biomacromol.*, **2013**, *14,* 291–296.
23. V. O. Ikem, A. Menner, T. S. Horozov, A. Bismarck, *Adv. Mater.*, **2010**, *22,* 3588–3592.
24. S. Kovačič, N. B. Matsko, G. Ferk, C. Slugovc *J. Mater. Chem. A*, **2013**, *1,* 7971–7978.
25. S. Wang, Z. Zhang, H. Liu, W. Zhang, Z. Qian, B. Wang, *Colloid.Polym. Sci.*, **2010**, *288,* 1031–1039.
26. (a) V. O. Ikem, A. Menner, A. Bismarck, *Soft Matter*, **2011**, *7,* 6571–6577 (b) L. L. C. Wong, V. O. Ikem, A. Menner, A. Bismarck, *Macromol. Rapid. Commun.*, **2011**, *32,* 1563–1568.
27. S. Kovačič, G. Ferk, M. Drofenik, P. Krajnc, *React. Funct. Polym.*, **2012**, *72,* 955–961
28. P. Y. Gac, D. Choqueuse, M. Paris, G. Recher, C. Zimmer, D. Melot, *Polym. Degrad. Stabil.*, **2013**, *98,* 809–817.
29. S. Kovačič, P. Krajnc, C. Slugovc, *Chem. Commun.*, **2010**, *46*, 7504–7506.
30. S. Kovačič, K. Jerabek, P. Krajnc, C. Slugovc, *Polym. Chem.*, **2012**, *3*, 325–328.
31. S. Kovačič, N. B. Matsko, K. Jerabek, P. Krajnc, C. Slugovc, *J. Mater. Chem. A*, **2013**, *1,* 487–490.
32. S. Kovačič, H. Kren, P. Krajnc, S. Koller, C. Slugovc, *Macromol. Rapid Commun.* **2013**, *34,* 581–587.
33. S. Kovačič, *Acta.Chim. Slov.*, **2013**, *60,* (2), 448–454.
34. A.-C. Knall, S. Kovačič, M. Hollauf, D. P. Reishofer, R. Saf, C. Slugovc, *Chem. Commun.* **2013**, *49*, 7325–7327.
35. R. Simons, S. N. Guntari, T. K. Goh, G. G. Qiao, S. A. Bateman, *J. Polym. Sci., Part A: Polym. Chem.*, **2012**, *50,* 89–97.
36. M. Yoonessi, H. Toghiani, C. U. Pittman. Jr., *J. Appl. Polym. Sci.,* **2006**, *102,* 2743–2751; W. Jeong, M. R. Kessler, *Chem. Mater.,* **2008**, *20,* 7060–7068.
37. V. Rudnev, D. Loveless, R. L. Cook, M. Black, *Handbook of Induction Heating*, Marcel Dekker Inc., New York, **2003.**
38. S. Ceylan, C. Friese, C. Lammel, K. Mazac, A. Kirschning, *Angew. Chem. Int. Ed.*, **2008**, *47,* 8950–8953
39. A. K. Gupta, M. Gupta, *Biomaterials,* **2005**, *26*, 3995–4021.
40. S. Gyergyek, D. Makovec, A. Mertelj, M. Huskic, M. Drofenik, *Colloids Surf. A*, **2010**, *366,* 113–119.
41. S. Kovačič, F. Preishuber-Pflügl, C. Slugovc, *Macromol. Mat. Eng.*, **2014**, DOI: 10.1002/mame.201300400
42. X. M. Wang, H. C. Gu and Z. Q. Yang, *J. Magn. Magn. Mater.*, **2005**, *293*, 334–340.

Povzetek

V tem strokovnem članku opisujem pripravo makroporoznih nanokompozitnih pen iz diciklopentadienskih HIP emulzij stabiliziranimi z γFe_2O_3/Fe_3O_4 nanodelci, t.i. Pickering emulzij in HIP emulzij stabiliziranimi s kombinacijo surfaktanta in nanodelcev. Tako pripravljene nanokompozitne pene smo primerjali s penami pripravljenimi iz HIP emulzij stabiliziranimi le s surfaktanti in ugotovili da se premer por spreminja in sicer od 7 ± 3 m do 950 ± 360 μm. V nadaljevanju smo nanokompozitne makroporzne pene funkcionalizirali z elementarnim bromom, ter raziskali vpliv bromiranja na samo lokacijo nanodelcev in sposobnost γFe_2O_3/Fe_3O_4 nanodelcev da ob prisotnosti zunanjega alternirajočega magnetnega polja proizvajajo toploto. V ta namen smo bromirano nanokompozitno peno izpostavili zunanjemu izmeničnemu magnetnem polju, ter ugotovili da se sposobnost segrevanje zmanjša za faktor 2.

Electronic Supplementary Information

Nanocomposite Foams from Iron Oxide Stabilized Dicyclopentadiene High Internal Phase Emulsions: Preparation and Bromination

Sebastijan Kovačič,[1,4]* Nadejda B. Matsko,[2] Gregor Ferk[3] and Christian Slugovc[1]

Scanning Electron Microscopy

Morphology investigations were done by scanning electron microscopy (SEMs were taken on a JWS-7515, JEOL Ltd. microscope). An average voids sizes were determined from SEM micrographs analysis after scanning. Therefore, the mean and the standard deviation were drawn by manual measurements of diameters from a population of at least 40 voids. From SEM images analysis, it is difficult to give a correct evaluation of the void size because the pores are inside the material and during sample sectioning the cavities which appear are at random distance from cavity centre. To get a better estimation of the real void diameter, it is necessary to introduce a statistical correction. Multiplication of the observed voids values from SEM images by statistical factor $2/3^{1/2}$ allows better estimation of real cavity diameters.

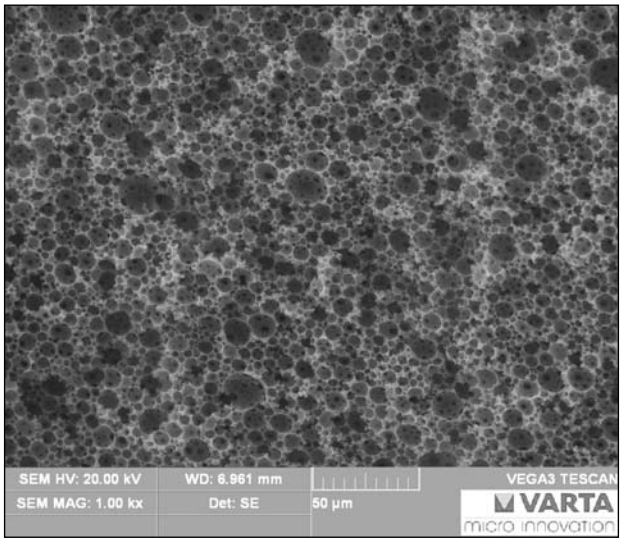

Figure S2. SEM image of nanocomposite foam **pDCPD-15w-1.5v** with 1.5 v% of surfactant in the precursor

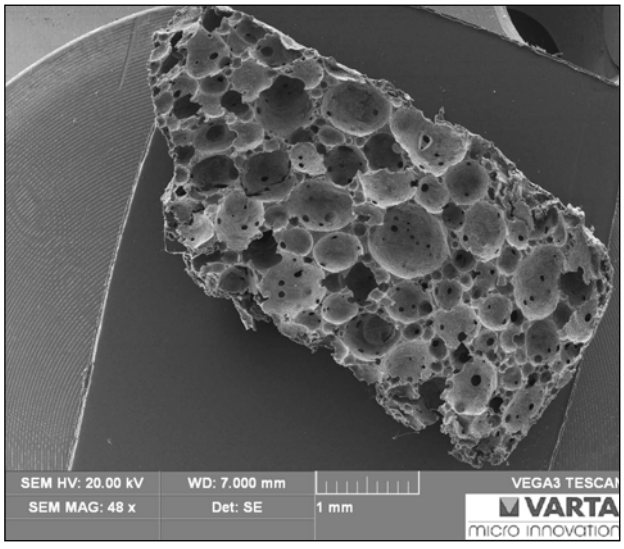

Figure S1. SEM image of nanocomposite foam **pDCPD-15w** without surfactant in the precursor

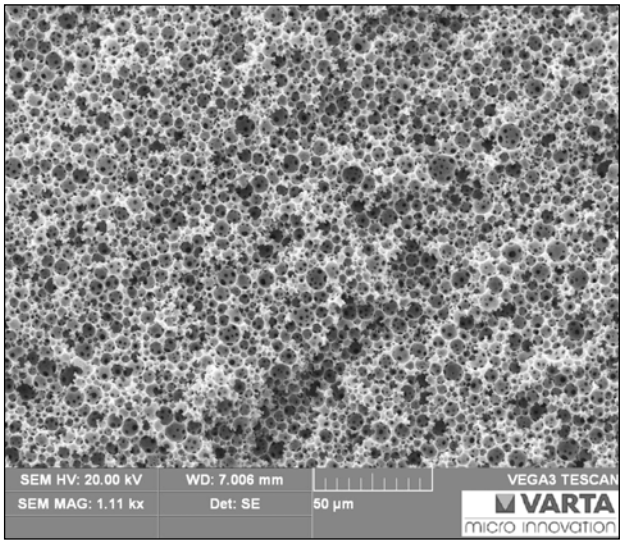

Figure S3. SEM image of nanocomposite foam **pDCPD-15w-10v** with 10 v% of surfactant in the precursor

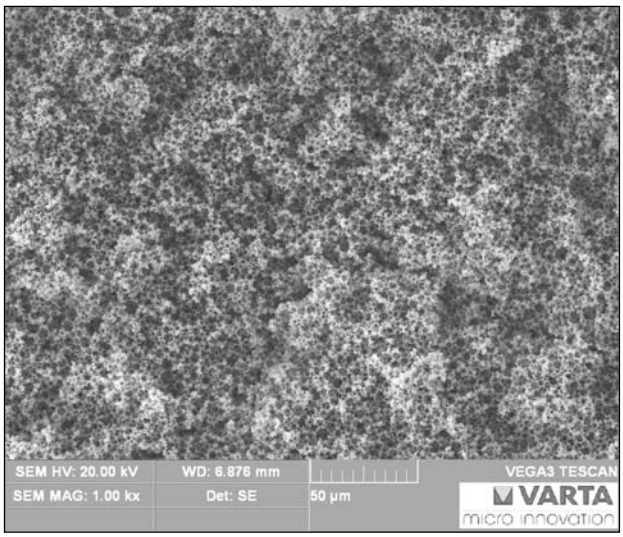

Figure S4. SEM image of **pDPCD-10v** foam stabilized without **FeO_x-NP**s and with 10 v% of surfactant

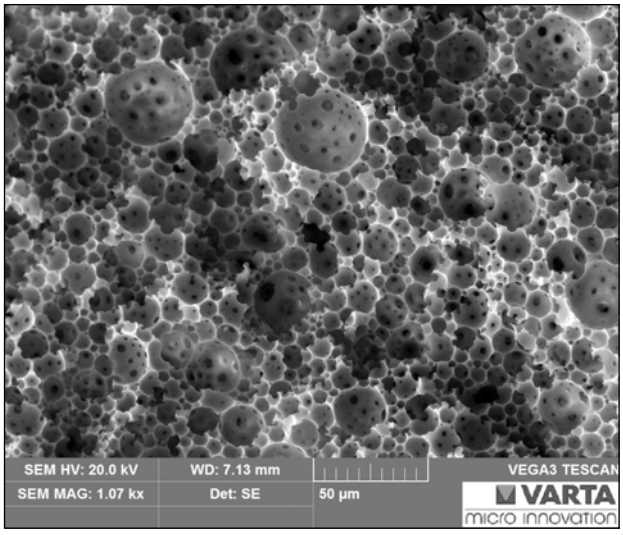

Figure S5. SEM image of **pDPCD-1.5v** foam stabilized without **FeO_x-NP**s and with 1.5 v% of surfactant

Induction Heating Tests of Nanocomposites

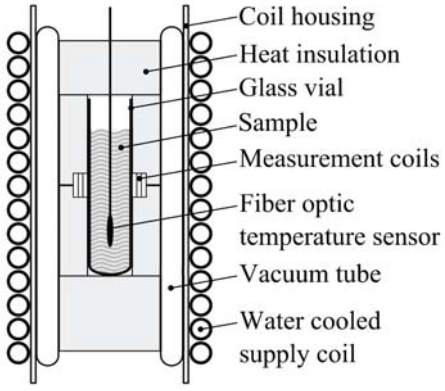

Figure S6. Conventionally built heating system

Thermo Gravimetric Analysis

TGA measurements were performed with a Netzsch Simultaneous Thermal Analyzer STA 449C (crucibles: aluminium from Netzsch). An oxygen flow of 50 mL/min was used in combination with a protective flow of helium of 8 mL/min. The heating rate until a final temperature of 550 °C was 10 °C/min.

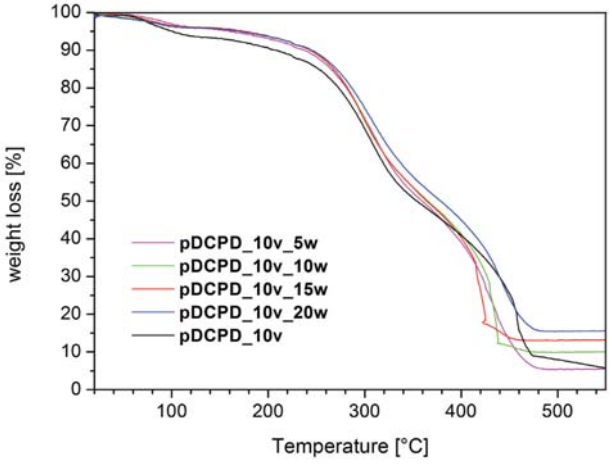

Figure S7. TGA of the composite foams performed in oxygen atmosphere

Bromination of Nanocomposite Foams

A piece of nanocomposite foam (4 g; 45.3 mmol of double bonds) was immersed in a THF (200 mL), where

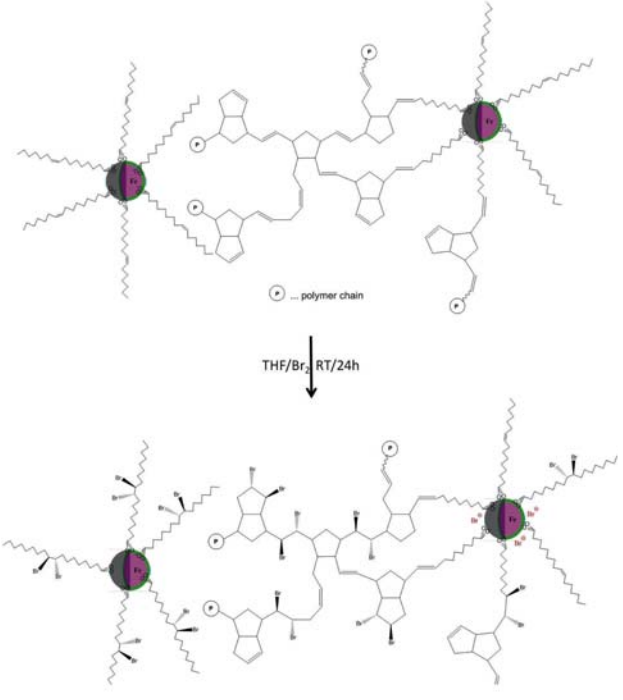

Figure S8. Tentative presentation of bromination protocol

to bromine (2.26 mL) was slowly added. The nanocomposite foam in solution of Br/THF was kept at room temperature for 24 h and subsequently washed with copious amounts of THF, acetone/THF and acetone. Finally, piece of nanocomposite foam was dried *in vacuo* at room temperature until constant weight.

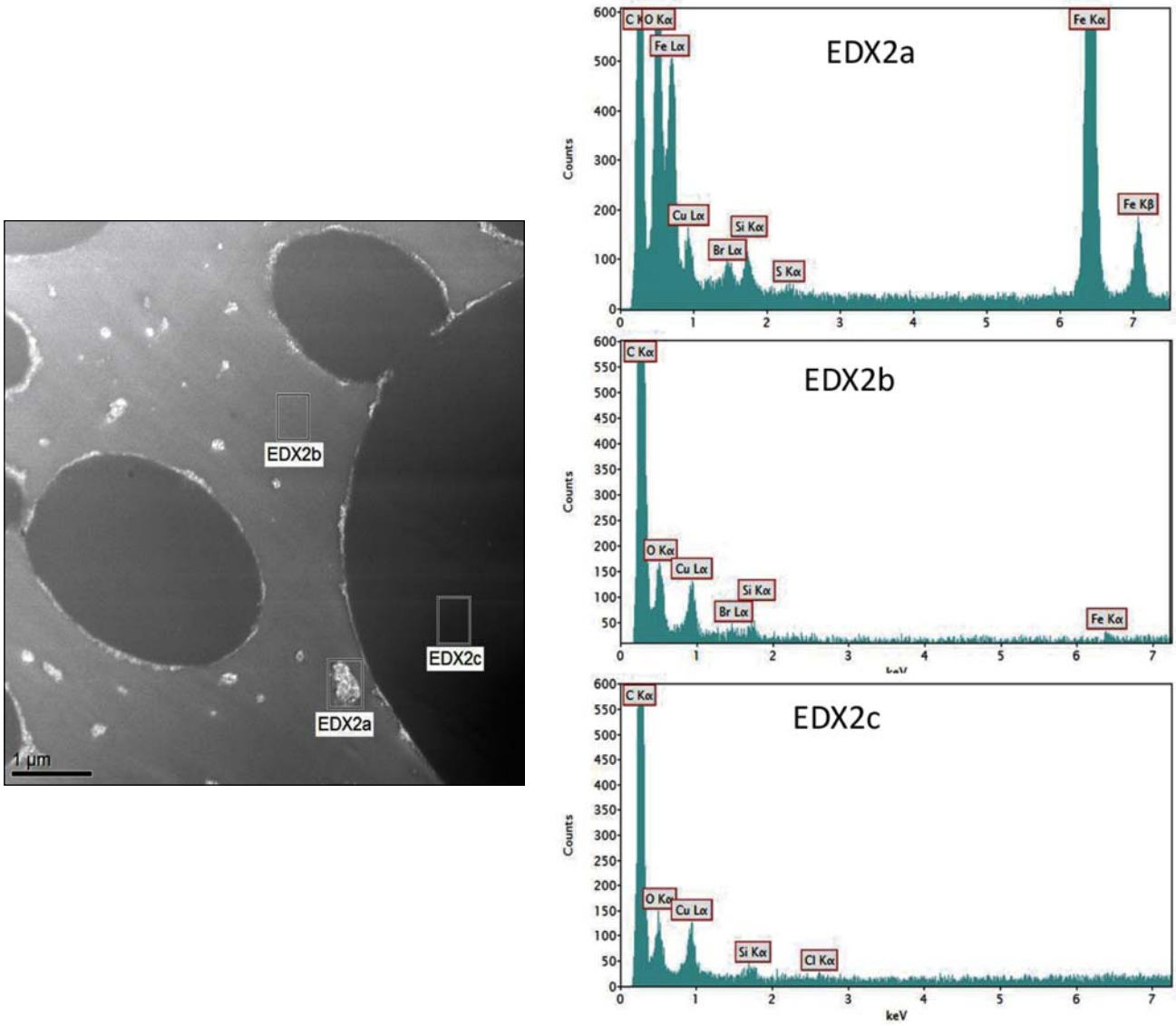

Figure S9. STEM and EDX analysis of brominated **pDCPD-15w-1.5v** nanocomposite foam